



<b>Experiment title:</b> Combined microrheology and dynamics study of concentrated colloidal hard-sphere suspensions near the glass transition volume fraction	<b>Experiment number:</b> SC-3776	
<b>Beamline:</b> ID10	<b>Date of experiment:</b> from: 30/10/2013 to: 05/11/2013	<b>Date of report:</b> 22/09/2014
<b>Shifts:</b> 18	<b>Local contact(s):</b> Yuriy Chushkin	<i>Received at ESRF:</i>
<b>Names and affiliations of applicants (* indicates experimentalists):</b> Paweł Kwaśniewski*, DESY, Hamburg, Joerg Hallmann, XFEL.EU, Hamburg; Anders Madsen*, XFEL.EU, Hamburg; Andrei Fluerasu*, BNL, NSLS II, NY 11973 Upton, USA		

## Report:

Initial measurements on the short-range attractive silica sample, showed its high radiation sensitivity, rendering the planned XPCS measurements impossible. By changing the experimental technique to X-ray Speckle Visibility Spectroscopy (XSVS) [1] we were able to overcome this difficulty, as well as measure sub-millisecond relaxation times, reaching beyond the limitations of standard “movie mode” XPCS, constrained by the maximum detector acquisition rate.

Stearyl alcohol coated silica particles undergo a reversible hard-sphere repulsive to short-range attractive phase transition upon cooling [2]. It can be tracked by looking at the azimuthally averaged SAXS profiles, as shown in Fig. 1 a) for a sample at 0.243 volume fraction, which shows an upturn of intensity at low  $q$  values for temperatures below 30 C, indicating particle aggregation due to attractive interactions. A plot of intensity averaged over pixels corresponding to  $q = (2 \pm 0.4) \times 10^{-3} \text{ \AA}^{-1}$ , shown in Fig. 1 b) and c), shows that the aggregates are quickly destroyed by the X-ray beam – the intensity decreases significantly after about 10 exposures on a single spot on the sample. Since the acquisition was repeated on several positions, a dataset can be constructed by taking only the first 10 frames from each spot. This data set displays no signs of radiation damage in the averaged intensity plot (panel d) and shows slower dynamics when compared to results obtained from a complete set of scattering patterns (see panel e).

Analysis of the visibility functions measured at  $T = 40 \text{ C}$  for a series of  $q$  values is presented in Fig. 2. For each  $q$  partition, marked on the averaged scattering image in panel a), intensity histograms were calculated for different exposure times, varying between 0.05 ms and 6.4 ms (panel b). Sub-ms exposure times were obtained by electronically limiting the detector pixel counters. It should be noted that this way the effective sample exposure is longer, due to the limited detector frame rate (1 kHz). Fits of photon count histograms with the negative binomial distribution function (Fig. 2, panel b) were then used to obtain the value of contrast as a function of exposure time (see Fig. 2, panel c). Since at this temperature the particles are expected to behave as hard spheres, the visibility functions are fitted with a model assuming simple exponential decay of the intermediate scattering function. The obtained dispersion relation, presented in panel d), departs from a quadratic  $q$  dependence,  $\Gamma = Dq^2$  (red solid line in panel d), upon approach to the  $S(q)$  peak position, displaying the de Gennes narrowing.

In conclusion, the results show that X-ray Speckle Visibility is a powerful technique, having the potential to overcome radiation damage in sensitive samples and to measure relaxation times shorter than ones accessible for the same detector with XPCS.

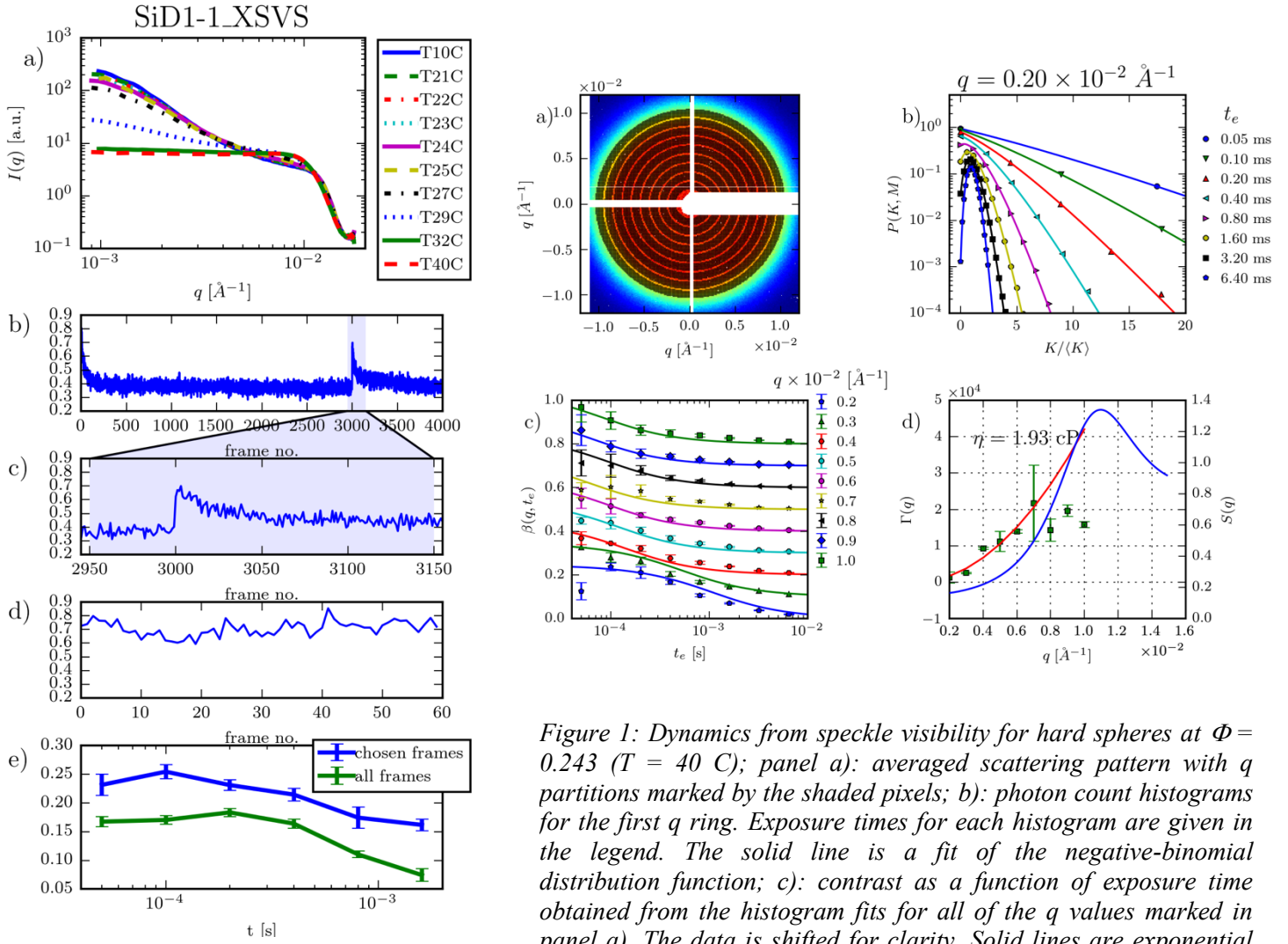


Figure 2: Panel a): azimuthally averaged SAXS profiles measured on the  $\Phi = 0.243$  sample at different temperatures. The remaining panels show data taken at 29 C. Panel b): intensity averaged over pixels corresponding to  $q = (2 \pm 0.4) \times 10^{-3} \text{ \AA}^{-1}$  plotted as a function of the acquired frame number. Panel c): magnification of the shaded area in the intensity plot in panel b). Panel d): intensity trace from a subset of the data, constructed by taking only first 10 frames acquired on a single spot on the sample. Panel e): comparison of two visibility functions: calculated on the complete data set (green curve) and on the chosen frames subset (blue curve).

Figure 1: Dynamics from speckle visibility for hard spheres at  $\Phi = 0.243$  ( $T = 40 \text{ C}$ ); panel a): averaged scattering pattern with  $q$  partitions marked by the shaded pixels; b): photon count histograms for the first  $q$  ring. Exposure times for each histogram are given in the legend. The solid line is a fit of the negative-binomial distribution function; c): contrast as a function of exposure time obtained from the histogram fits for all of the  $q$  values marked in panel a). The data is shifted for clarity. Solid lines are exponential decay fits of the visibility functions; d): Green points: relaxation rate obtained from visibility function fits as a function of  $q$ , fitted with a quadratic model (red line). Departure of the data points from the model in the vicinity of the  $S(q)$  peak (solid blue line) is a signature of the de Gennes narrowing.

## References

- [1] Li, L., Kwaśniewski, P., Orsi, D., Wiegart, L., Cristofolini, L., Caronna, C., and Fluerasu, A. ‘Photon Statistics and Speckle Visibility Spectroscopy with Partially Coherent X-rays’. *Accepted to J. Synch. Rad.* (2014).
- [2] Sztucki, M., T. Narayanan, G. Belina, A. Moussaïd, F. Pignon, and H. Hoekstra. ‘Kinetic Arrest and Glass-Glass Transition in Short-Ranged Attractive Colloids’. *Physical Review E* 74 (2006): 051504.